



# Effect of amorphous rice husk silica addition on the structure of asphalt composite

Simon SEMBIRING<sup>1,\*</sup>, Agus RIYANTO<sup>1</sup>, Rudy SITUMEANG<sup>2</sup>, Zipora SEMBIRING<sup>2</sup>, Nita SUSANTI<sup>1</sup>, and Iqbal FIRDAUS<sup>1</sup>

<sup>1</sup> Department of Physics, Faculty of Mathematics and Natural Sciences, Lampung University, Street. Prof. Soemantri Brojonegoro No.1 Bandar Lampung, 35145, Indonesia

<sup>2</sup> Department of Chemistry, Faculty of Mathematics and Natural Sciences, Lampung University, Street Prof. Soemantri Brojonegoro No. 1 Bandar Lampung, 35145, Indonesia

\*Corresponding author e-mail: simon.sembiring@fmipa.unila.ac.id

## Received date:

24 February 2020

## Revised date

19 August 2020

## Accepted date:

23 August 2020

## Keywords:

Rice husk;  
Silica;  
Asphalt;  
Microstructure;  
Structure

## Abstract

In this study, modified asphalt composites were produced by adding silica extracted from rice husk. The mass ratios of asphalt to silica are 1:0, 1:1.6, 1:1.8, and 1:2 and calcined at the temperature of 150°C for 6 h. The structural and microstructural characteristics of asphalt composites were examined by x-ray diffraction (XRD), Scanning Electron Microscopy/Energy Dispersive x-ray (SEM-EDX) Spectroscopy and Differential Thermal Analysis (DTA-TGA), respectively. The XRD study revealed that the major phases were carbon and amorphous silica. The surface morphology of asphalt without silica addition presents a cluster of larger size than the cluster of asphalt with an addition of silica. The addition of silica significantly increased the thermal stability of the asphalt due to the formation of a physically cross-linked silica network structure. DTA/TGA analyses produced that temperature decomposition increased with the increasing silica addition from 230°C to 315°C. Based on these characteristics, the samples are considered for the roof material, suggesting their potential use in substitute lightweight steel roof devices.

## 1. Introduction

Asphalt has a chemical composition with unique viscosity and elasticity properties that is very temperature dependent, so it has been widely used for roofing, road pavement and sealing applications due to its waterproof and good bonding properties. In the residential roof industry, asphalt generally requires the process of blowing air to reach the right softening, and penetration points. Besides that, asphalt is formed from hydrocarbon compounds with a chemical composition of 80% carbon, 10% hydrogen, 6% sulfur, and residual nitrogen and oxygen. With thermal treatment, asphalt can be converted into an adhesive liquid which makes it easy to mix with other materials. In the cooling process, the asphalt becomes waterproof, sticky, and strong. Due to severe temperature susceptibility, the application of asphalt is limited. Therefore, it should be considered in a number of applications where structural and micro-changes can affect the physical, thermal and mechanical properties of asphalt. Some researchers have tried changing the characteristics of asphalt to improve functionality and benefits by using various polymers such as styrene-butadiene rubber [1], waste crumb rubber [2], used waste rubber and plastic [3], waste polyethylene [4]. Based on previous research shows that modified asphalt not only has good durability, and resistance to crack deformation, but also can maintain good stability at high and low temperature performance [5-6].

Several materials have the possibility to be utilized to modify asphalt, such as, hydrated lime, plastic powders, or polymerized powders.

One of the inorganic additives of materials that have been used intensively is silica. Due to the high surface area, and strong adsorption, silica has the potential to prepare asphaltic materials with desirable properties. For example, Enieb and Diab, 2017 [7] found that the viscosity and the softening point of asphalt increased significantly with increased silica from 2 to 4%. When silica fume was implemented as additives to asphalt cement, it was noticed that penetration decreased, softening point increased [8-9]. In addition, literature studies showed that silica can enhance the anti-aging, fatigue cracking, rutting resistance, and anti-stripping properties of the asphalt [10]. Kai *et.al*, 2018 [11] observed the thermal stability of modified asphalt through the thermal analysis. Their results suggested that the high-temperature performance of asphalt improved with the increase of the silica fume content. Also, the addition of the silica fume could increase the contraction coefficient of the mixture [12].

Rice husk as agricultural waste is known to contain considerable amounts of silica, which can be extracted by relatively simple methods to obtain high purity, and active silica. Number of researchers [13-15] concluded that pure silica can be extracted with purity in the 94-98% range present as amorphous and reactive. In some references, amorphous silica from rice husk has been used for the preparation of various silica-based materials, such as the production of nano-silica [16-19], zeolite [20-21], nanoporous carbon [22-23], mullite [24-25], forsterite [26-27], nepheline [28], and cordierite [29].

This work presents the effect of amorphous rice husk silica addition on the crystallization properties of modified asphalt, which

can be developed for application as substitute lightweight steel roof devices. To obtain detailed information about some modified asphalt characteristics with the addition of silica was analyzed using XRD, SEM/EDX, and DTA/TGA.

## 2. Experimental

### 2.1 Materials

The matrix asphalt used in this experiment was obtained from Buton refinery, Southeast Sulawesi Province, Indonesia, and the modifiers were made of rice husk silica. The chemicals used are 5% NaOH, 5% KOH, 5% HCl, and absolute alcohol ( $C_2H_5OH$ ) purchased from Merck (KGaA, Darmstadt, Germany), and deionized/distilled water.

### 2.2 Preparation of composite- modified asphalt

Firstly, to obtain silica, rice husk was extracted by following the literature in previous studies [27]. The sol obtained are dripped with 5% HCl solution until the sol turn completely to the gel. The gel was dried at  $110^\circ C$  for eight hours and then ground into a powder by mortar and sieved to 200 meshes. Typically, 50 g of solid asphalt is melted by heating at  $100^\circ C$  and mixed with powdered silica using a shear mixer at a rate of 125 rpm for 4 h. Finally, calculated the quantity of silica is added under stirring to asphalt to provide the asphalt and silica as a mass ratio of 1:0, 1:1.6, 1:1.8 and 1:2. Furthermore, the powder was pressed into the form of a cylinder pellet with a pressure of  $2 \times 10^4 \text{ N}\cdot\text{m}^{-2}$ . The pellet is then calcined at  $150^\circ C$  for 6 h.

### 2.3 Characterization

Collection of XRD data was conducted with an automated Shimadzu XD-610 X-ray diffractometer at the National Agency for Nuclear Energy (BATAN). The XRD data were taken with  $CuK\alpha$  radiation ( $\lambda=1.5406 \text{ nm}$ ) at 40 kV and 30 mA in the range of  $2\theta=5-80^\circ$ , with a step size of 0.02, counting time 1s/step and  $0.15^\circ$  receiving slit. Microstructural analysis of the polished and etched samples was undertaken by SEM Philips-XL. Thermal analysis was performed using DTA Merck Setaram Tag 24 S, under the nitrogen atmosphere with a constant heating rate of  $3^\circ C\cdot\text{min}$ , at the temperature range of  $30^\circ C$  to  $800^\circ C$ .

## 3. Results and discussion

### 3.1 Structure characteristic of modified asphalt

Characterization of the samples using the XRD technique was conducted to evaluate the crystallographic structure of the sample. The spectra of the samples are shown in Figure 1(a-d). Figure 1(a) shows the spectrum of asphalt without the addition of silica and Figure 1(b-d) show the patterns of the modified asphalt with the different silica addition.

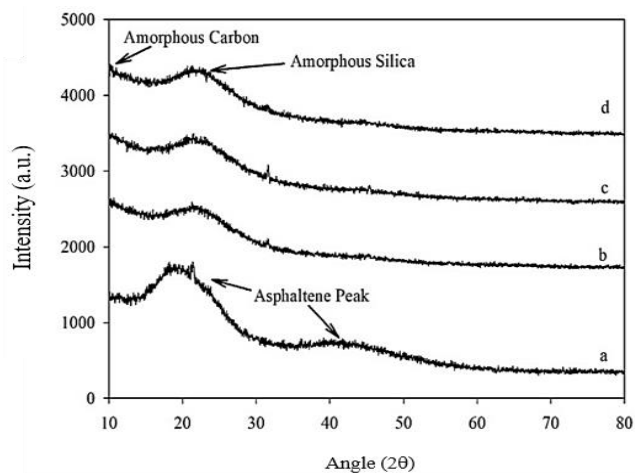


**Figure 1.** X-ray diffraction patterns of samples with ratio of asphalt to silica using  $CuK\alpha$  radiation, (a) Asphalt without silica, (b) 1:1.6, (c) 1:1.8, and (d) 1:2.

As can be seen, the diffraction peak intensity of the sample presented in Figure 1(a) was located at approximately  $18-25^\circ$  and  $43^\circ$  values of  $2\theta$ , amorphously indicating it came from crystalline asphaltenes, as supported by the previous study [30-31]. The peak asphaltene appears at around  $2\theta = 20^\circ$  because of the aliphatic chains or condensed saturated rings. The peak formed at approximately  $2\theta = 23.20^\circ$  is known as multilayered graphene [32]. The formation of the multilayered graphene is emerged by staging the aromatic molecules existing in the asphaltenic structure. At the  $2\theta$  value ( $42.52^\circ$ ), a weak band is formed, which is due to the influence of nearest neighbors in the ring structure [33-34].

The diffraction patterns in Figure 1(b-d) indicate that the samples with additions of silica were still amorphous, marked by the existence of two broad peaks, most likely resulted from accumulation of carbon peak position ( $2\theta = 10^\circ$ ) and silica peak position ( $2\theta = 21.8^\circ$ ). The presence of carbon and silica is in accordance with the results of EDX analyses, described in the following section. The detection of carbon and silica demonstrates that significant transformation of amorphous asphaltenes has taken place. However, the change in the peak diffraction is a result of strong molecular interactions between asphalt and silica through exfoliation and intercalation process in the samples.

### 3.2 Microstructure characteristic of modified asphalt

The surface images of the samples with the different silica content obtained from SEM analyses are shown in Figure 2(a-d). The results obtained from SEM analyses are supported by the composition of the samples as indicated by the EDX results shown in Figure 3(a-d) and Table 1. The sample without the silica addition (Figure 2(a)) is marked by the presence of large clusters without evident grain boundaries, most likely deriving from the arrangement of asphalt structures as supported XRD result (Figure 1(a)) and a high amount (91.77%) of the carbon was obtained in asphalt without silica (Table 1). In this particular sample, the prominent particles are most likely the carbon present as larger particles, suggesting that the sample is dominated by carbon.

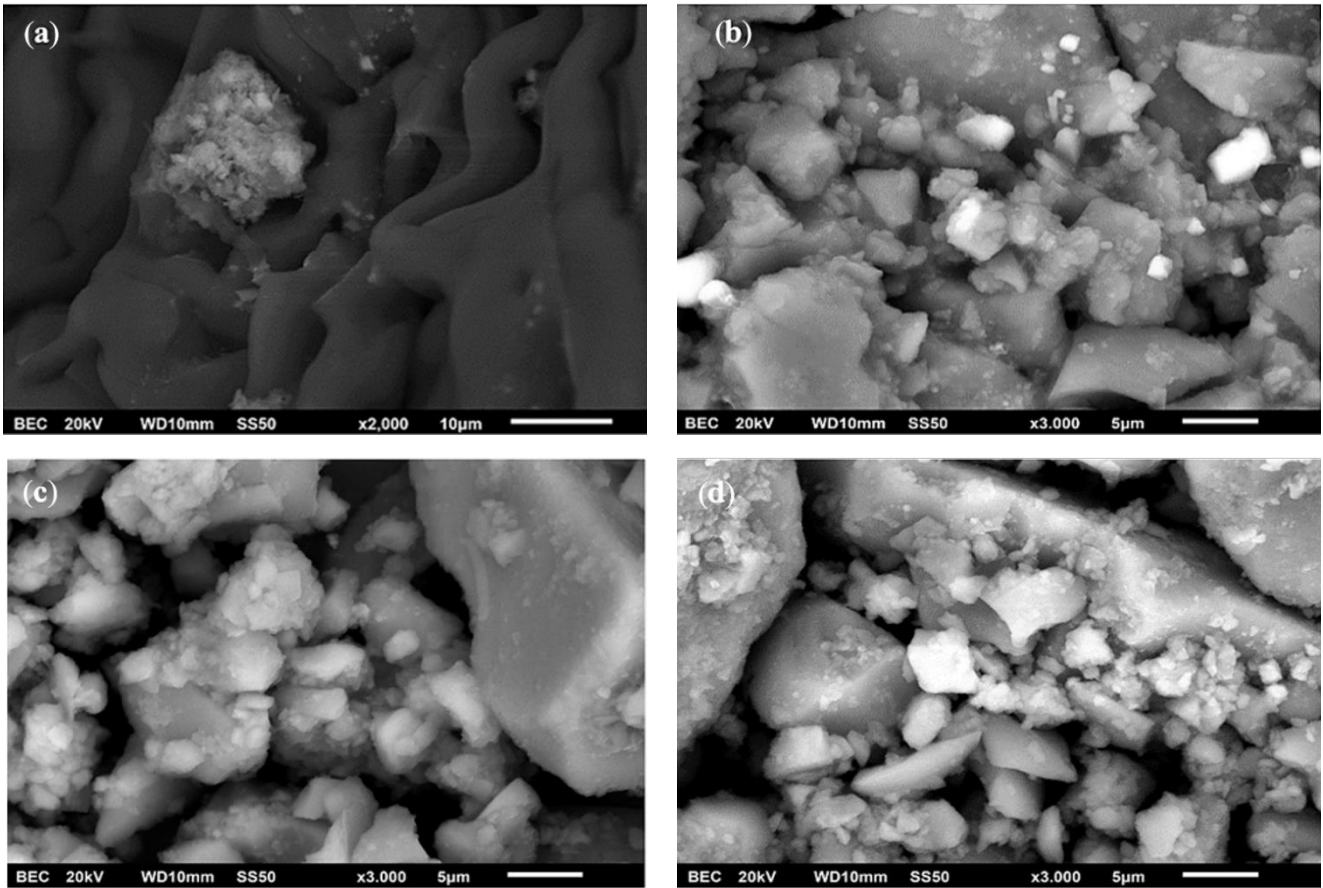


Figure 2. The scanning electron microscopy (SEM) images of the samples with ratio of asphalt to silica (a) Asphalt without silica, (b) 1:1.6, (c) 1:1.8, and (d) 1:2.

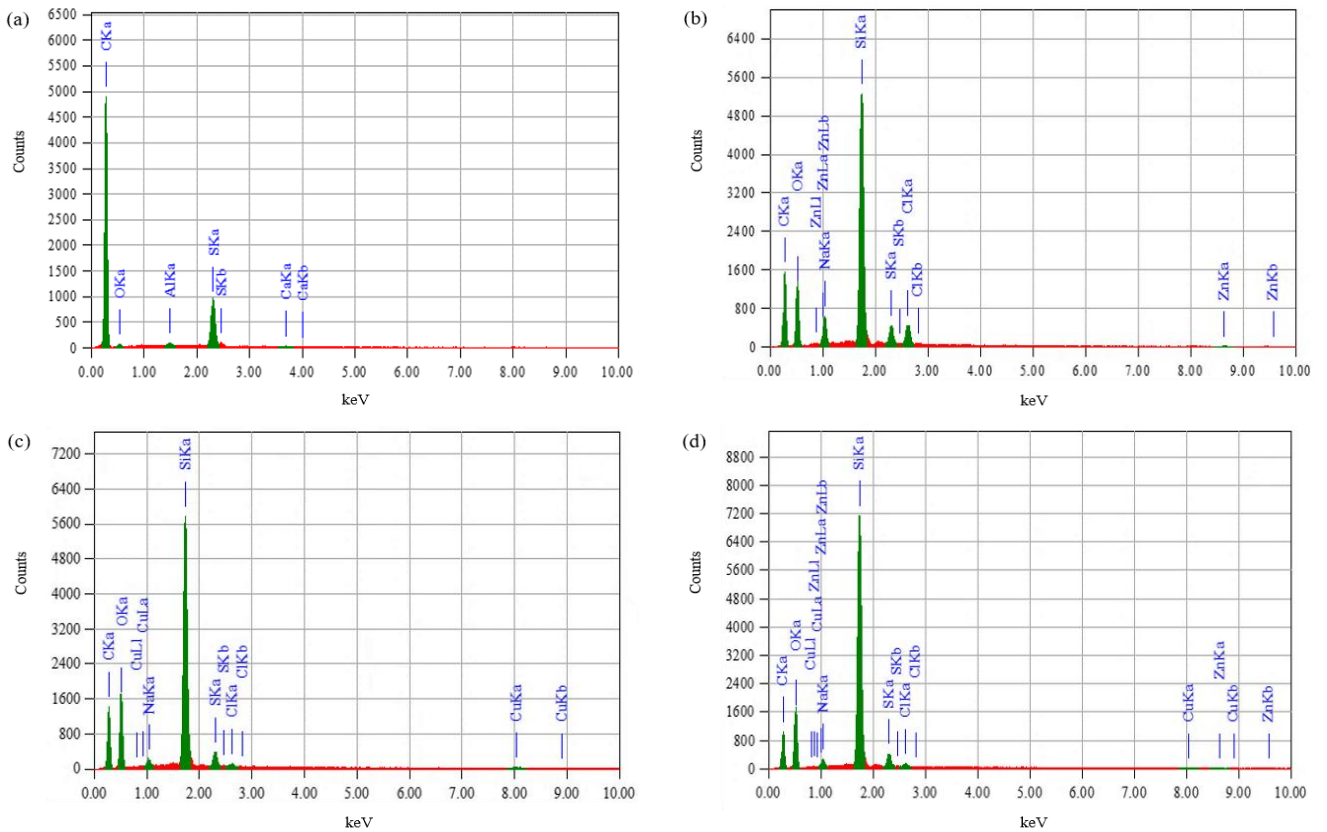


Figure 3. The EDX spectra of the samples prepared at different ratio of asphalt to silica (a) asphalt without silica, (b) 1:1.6, (c) 1:1.8, and (d) 1:2.

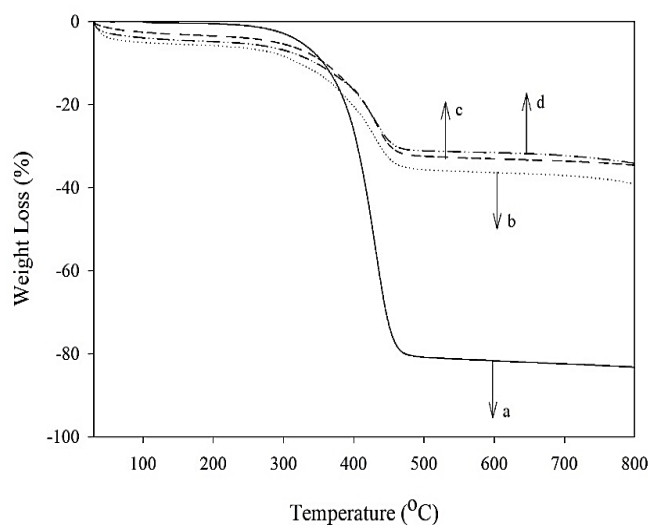
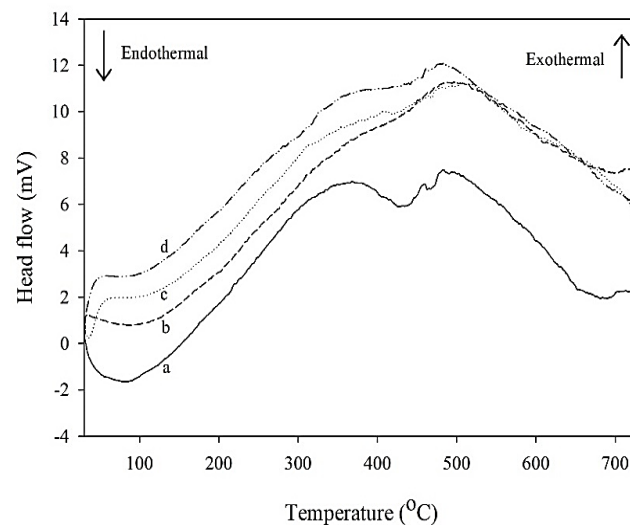
**Table 1.** Composition of samples according to EDX spectra.

Sample	Carbon (wt%)	Na <sub>2</sub> O (wt%)	SiO <sub>2</sub> (wt%)	SO <sub>3</sub> (wt%)	Cl (wt%)
Asphalt	91.77	-	-	8.47	-
1:1.6	63.64	2.86	28.47	3.47	1.56
1:1.8	61.54	0.89	34.05	3.26	0.27
1:2	53.19	1.22	41.66	3.59	0.34

The micrographs presented in Figure 2(a-d) show the significant effect of silica addition to the size and distribution of the particles on the surface. As shown in Figure 2(a-d), the surface morphologies of the samples are marked by the existence of particles with different grain sizes and distribution. The microstructure of the sample without the addition of silica (Figure 2(a)) displays quite different characteristics to those of the samples with 1.6, 1.8 and 2 g silica addition (Figure 2(b-d)). The EDX data presented in Table 1 clearly indicated the significant effect of silica addition to the composition of the samples. As can be seen, the sample without silica only contained a very large amount (91.77%) of carbon, and the percentage of this element decreased sharply to 53.19% in the sample with the addition of silica up to 2 g. Meanwhile, the sample with the silica addition of 1.6 g contained 28.77% of silica and increased to 41.66% with silica addition up to 2 g. The surfaces of the samples containing additional silica of 1.6, 1.8 and 2 g (Figure 2 (b-d)) are marked by fine grains of silica structure cover several large grains of asphalt structure, which according to XRD results (Figure 1(b-d)) are composed of carbon and silica. Due to the agglomeration of silica, the silica group reacted with the asphalt, and the size of the silica group became smaller. The presence of carbon and silica phases in the last three samples suggest that the silica phase continued to change and allowed the particle arrangement, leading to initiation of the formation of asphalt composite. Furthermore, the SEM image indicates that the sample is denser with the addition of 2 g silica, which leads to a compact shape in accordance with the results of TGA/DTA analyses, described in the following section.

### 3.3 Thermal characteristic of modified asphalt

The thermal characteristics of modified asphalt are an important property to be considered in the analysis of the structural characteristics of asphalt. In this study, thermal characteristics of the samples were evaluated by analyzing the samples with (TGA/DTA). The TGA thermograms of the samples with different rice husk silica addition are compiled from Figure 4 and DTA results are shown in Figure 5. The TGA results presented in Figure 4 indicate the existence of four temperature zones, indicating the patterns of weight loss of the samples. The TGA results emphasize two major mass loss stages for all samples, e.g. (i) very small weight loss (Figure 4 and Table 2) occurs in the temperature range of 30-300°C, mainly due to the volatility of asphaltene components such as saturation and decomposition components of naphthene aromatic fractions asphaltene [35-36], and (ii) weight loss starts at 300°C and ends at 500°C, the results show a very sharp weight loss. Weight loss occurs due to asphaltene decomposition and silica crystallization, supported by endothermic peak presence at 500°C in DTA thermogram as shown in Figure 5. From 300 to 500°C, the rate of weight loss decreases sharply as temperature increases, and after 500°C, the samples, practically have reached a stable state, the TGA curve became flat as displayed in Figure 4. The maximum endothermic temperature at 500°C from the DTA curve shows that the sample has achieved thermal stability as demonstrated by others [37]. This means that silica particles and asphalt mixed homogeneously to form a compact blend.

**Figure 4.** TGA Thermograms of the samples with ratio of asphalt to silica, (a) asphalt without silica, (b) 1:1.6, (c) 1:1.8, and (d) 1:2.**Figure 5.** DTA Thermograms of the samples with ratio of asphalt to silica, (a) asphalt without silica, (b) 1:1.6, (c) 1:1.8, and (d) 1:2.

**Table 2.** Summary of TGA properties results for all samples.

Sample	Onset temp (°C)	Max Temp (°C)	Weight loss 30-300°C (%)	Weight loss 300-500°C (%)	Residue after 500°C (%)
Asphalt	230	453	0.5	79.9	19.6
1:1.6	267	463	6.7	35.6	57.7
1:1.8	283	473	4.9	30.8	64.3
1:2	315	497	5.9	29.3	64.8

#### 4. Conclusions

This study demonstrated that asphalt composite was successfully prepared using rice husk silica as raw material. Rice husk silica addition from 1.6 to 2 g revealed the formation of carbon and silica amorphous from interaction between asphalt and silica. SEM analysis with the addition of silica indicates clearly that the scattered silica covering the asphalt with a small grain size found in the asphalt ratio to silica is 1:2. Structure transformation was observed to result in the change of the characteristics of the samples which related to increase temperature decomposition. Also, the result presents that the asphalt composite with a ratio of 1:2 is suitable for the design of roof materials with the highest temperature decomposition. Based on these characteristics, the samples are considered for the roof material, suggesting their potential use in substitute lightweight steel roof devices.

#### Acknowledgments

The authors wish to thank and appreciate Ministry of Research, Technology, and High Education, Directorate General of Strengthening Research and Development, the Republic of Indonesia for research funding provided through the *Decentralization Research/ Basic research university/PDUPT Grant/UN26/KU/2020*

#### References

- [1] F. Zhang, and J.Y. Yu, "The research for high-performance SBR compound modified asphalt," *Construction and Building Materials*, vol. 24, pp. 410-418, 2010.
- [2] Y. Yang, and Y. Cheng, "Preparation and performance of asphalt compound modified with waste crumb rubber and waste polyethylene," *Advances in Materials Science and Engineering*, vol. 2016, pp.1-6, 2016.
- [3] C.Q. Fang, L.N. Jiao, and J.B. Huetal, "Viscoelasticity of asphalt modified with packaging waste expended polystyrene," *Journal of Materials Science and Technology*, vol. 30, pp. 939-943, 2014.
- [4] S. Hinislioglu and E. Agar, "Use of waste high density polyethylene as bitumen modifier in asphalt concrete mix," *Materials Letters*, vol. 58, pp. 267-271, 2004.
- [5] H. Wang, Z.P. You, J.L. Mills-Beale, and P.W. Hao, "Laboratory evaluation on high temperature viscosity and low temperature stiffness of asphalt binder with high percent scrap tire rubber," *Construction and Building Materials*, vol. 26, pp. 583-590, 2012.
- [6] M. Arabani, S.M. Mirabdolazimi, and A.R. Sasani, "The effect of waste tire thread mesh on the dynamic behaviour of asphalt mixtures," *Construction and Building Materials*, vol. 24, pp. 1060-1068, 2010.
- [7] M. Enieb and A. Diab, "Characteristics of asphalt binder and mixture containing nanosilica," *International Journal of Pavement Research and Technology*, vol. 10, pp. 148-157, 2017.
- [8] S.I. Sarsam, "Effect of nano materials (Silica Fumes and Hydrated lime) on rheological and physical properties of asphalt cement," in the Third International Scientific Conference, ME3-CM01, University of Babylon-Hilla-Babylon- IRAQ, 2015.
- [9] H. Ezzat, S. El-Badawy, A. Gabr, I.Z. El-Saaid, and T. Breakah, "Evaluation of asphalt binders modified with nanoclay and nanosilica," *Procedia Engineering*, vol. 143, pp. 1260-1267, 2016.
- [10] J. Yang, and S. Tighe, "A review of advances of nanotechnology in asphalt mixtures," *Procedia-Social and Behavioral Sciences*, vol. 96, pp. 1269-1276, 2013.
- [11] C. Kai, W. Xu, D. Chen, and F. Huimin, "High- and low-temperature properties and thermal stability of silica fume/SBS composite-modified asphalt mortar," *Advances in Materials Science and Engineering*, vol. 2018, pp. 1-8, 2018.
- [12] Y.Q. Tan, L.Y. Shan, and J. Fang, "Anti-cracking mechanism of diatomite asphalt and diatomite asphalt mixture at low temperature," *Journal of Southeast University*, vol. 25, pp. 74-78, 2009.
- [13] M.M. Haslinawati, K.A. Matori, Z.A. Wahab, H.A.A. Sidek, A.T. Zainal, "Effect of temperature on ceramic from rice husk ash," *International Basic & Applied Science*, vol. 09, pp. 22-25, 2009.
- [14] E. Rafieel, S. Shahebrahimi, M. Feyzil, and M. Shaterzadeh, "Optimization of synthesis and characterization of nanosilica produced from rice husk (a common waste material)," *International Nano Letters*, vol. 2, pp. 1-8, 2012.
- [15] B.I. Ugheoke and O.A. Mamat, "A Novel method for high volume production of nano silica from rice husk: process development and product characteristics," *International Material Engineering Innovation*, vol. 3, pp. 139-155, 2012.
- [16] K. Amutha, R. Ravibaskar and G. Sivakumar, "Extraction, synthesis and characterization of nanosilica from rice husk ash," *International nano Technology and Application*, vol. 4 pp. 61-66, 2010.
- [17] L.N.A. Tuan, L.T.K. Dung, L.D.T. Ha, N.Q. Hien, D.V. Phu, B.D. Du, "Preparation and characterization of nanosilica from rice husk ash by chemical treatment combined with calcination," *Vietnam Journal of Chemistry*, vol. 55, pp. 446-455, 2017.

- [18] T.H. Liou and C.C. Yang, "Synthesis and surface characteristics of nanosilica produced from alkali-extracted rice husk ash," *Material Science Engineering*, vol. B 176, pp. 521-529, 2011.
- [19] V.B. Carmona, R.M. Oliveira, W.T.L. Silva, L.H.C. Mattoso, and J.M. Marconcini, "Nanosilica from rice husk: extraction and characterization," *Industry Crops and Production*, vol. 43, pp. 291-296, 2013.
- [20] M.M. Mohamed, F.I. Zidan and M. Thabet, "Synthesis of ZSM-5 zeolite from rice husk ash: characterization and implications for photocatalytic degradation catalysts," *Micropore and Mesopore Material*, vol. 108, pp. 193-203, 2008.
- [21] G. Zahra, and Y. Habibollah, "Preparation and characterization of nanozeolite NaA from rice husk at room temperature without organic additives," *Nano Material*, pp. 1-8, 2011.
- [22] A. Mehta, and R.P. Ugwekar, "Extraction of silica and other related products from rice husk," *International Engineering Research and Application*, vol. 25, pp. 43-48, 2015.
- [23] H. Xu, B. Gao, H. Cao, X. Chen, L. Yu, K. Wu, L. Sun, X. Peng, and J. Fu, "Nanoporous activated carbon derived from rice husk for high performance super capacitor," *Nano Material*, pp. 1-7, 2014.
- [24] M.F. Serra, M.S. Conconia, M.R. Gaunaa, G. Suáreza, E.F. Aglietti, and N.M. Rendtorff, "Mullite ( $3\text{Al}_2\text{O}_3 \cdot 2\text{SiO}_2$ ) ceramics obtained by reaction sintering of rice husk ash and alumina, phase evolution, sintering and microstructure," *Asian Ceramic Society*, vol. 4, pp. 61-77, 2016.
- [25] S. Sembiring, W. Simanjuntak, P. Manurung, D. Asmi and I.M. Low, "Synthesis and characterisation of gel-derived mullite precursors from rice husk silica," *Ceramic International*, vol. 40, pp. 7067-7072, 2014.
- [26] S.K.S. Hossain, L. Mathur, P. Singh, M.R. Majhi, "Preparation of forsterite refractory using highly abundant amorphous rice husk silica for thermal insulation," *Asian Ceramic Society*, vol. 5, pp. 82-87, 2017.
- [27] S. Sembiring, A. Riyanto, W. Simanjuntak and R. Situmeang, "Effect of MgO-SiO<sub>2</sub> ratio on the forsterite ( $\text{Mg}_2\text{SiO}_4$ ) precursors characteristics derived from amorphous rice husk silica," *Journal of Oriental Chemistry*, vol. 33, pp. 186-192, 2017.
- [28] F. Andreola, M.I. Martín, A.M. Ferrari, I. Lancellotti, Bondioli, J.M. Rincón, M. Romero, and L. Barbieri, "Technological properties of glass-ceramic tiles obtained using rice husk ash as silica precursor," *Ceramic International*, vol. 39, pp. 5427-5435, 2013.
- [29] S. Sembiring, W. Simanjuntak, R. Situmeang, A. Riyanto, and K. Sebayang, "Preparation of refractory cordierite using amorphous rice husk silica for thermal insulation purposes," *Ceramic International*, vol. 42, pp. 8431-8437, 2016.
- [30] S.A.M. Hesp, I. Serban, and J.W. Shirokoff, "Reversible aging in asphalt binders," *Energy Fuels*, vol. 21, pp. 1112-1121, 2007.
- [31] P.J. Yoo, and T. Yun, "Micro-heterogeneous modification of an asphalt binder using a dimethylphenol and high-impact polystyrene solution," *Construction Building Material*, vol. 49, pp. 77-83, 2013.
- [32] N. Nciri, J. Kim, N. Kim, and N. Cho, "An In-Depth Investigation into the physicochemical, thermal, microstructural, and rheological properties of petroleum and natural asphalts," *Materials*, vol. 9, pp. 1-20, 2016.
- [33] V.S. Babu, L. Farinash, and M.S. Seehra, "Carbon in diesel particulate matter: Structure, microwave absorption, and oxidation," *Journal of material research*, vol. 10, pp. 1075-1078, 1995.
- [34] V.S. Babu, and M.S. Seehra, "Modeling of disorder and X-ray diffraction in coal-based graphitic carbons," *Carbon*, vol. 34, pp. 1259-1265, 1996.
- [35] M. Juan, M. Jiménez, C.Q. Luis, and R. Carmen, "Characterization of petroleum bitumens and their fractions by thermogravimetric analysis and differential scanning calorimetry," *Fuel*, vol. 75, pp. 1691-1700, 1996.
- [36] C.K. Radhakrishnan, A. Sujith, and G. Unnikrishnan, "Thermal behaviour of styrenebutadiene rubber/poly(ethylene-co-vinylacetate) blends TG and DSC analysis," *Journal of Thermal Analyses Calorimetre*, vol. 90, pp. 191-199, 2007.
- [37] C.H. Xu, Y.Z. Lin, J.M. Xiang, and Q.H. Wang, "Application of DTA and DTG methods in the study of thermal stability of cis-1,4-polybutadiene rubbers," *China Synthesis Rubber Industry*, vol. 8, pp. 419-422, 1985.